ω_1 or ω_2. For the following, we consider plane waves which propagate in a direction without walk-off so we consider a single wave frame; the energy distribution is assumed to be flat, so the three beams have the same radius w_o.

1.7.3.3.4.1. *SFG ($\omega_1 + \omega_2 = \omega_3$) with undepletion at ω_1 and ω_2*

The resolution of system (1.7.3.22) with $E_1(X, Y, 0) \neq 0$, $E_2(X, Y, 0) \neq 0$, $\partial E_1(X, Y, Z)/\partial Z = \partial E_2(X, Y, Z)/\partial Z = 0$ and $E_3(X, Y, 0) = 0$, followed by integration over (X, Y), leads to

$$P^{\omega_1}(L) = (T^{\omega_1})^2 P^{\omega_1}(0) \tag{1.7.3.81}$$

$$P^{\omega_2}(L) = (T^{\omega_2})^2 P^{\omega_2}(0) \tag{1.7.3.82}$$

$$P^{\omega_3}(L) = BP^{\omega_1}(0)P^{\omega_2}(0)\frac{L^2}{w_o^2}\sin c^2\frac{\Delta k \cdot L}{2} \tag{1.7.3.83}$$

with

$$B_{\rm SFG} = \frac{72\pi}{\varepsilon_o c}\frac{2N-1}{N}\frac{d_{\rm eff}^2}{\lambda_\omega^2}\frac{T^{\omega_3}T^{\omega_1}T^{\omega_2}}{n^{\omega_3}n^{\omega_1}n^{\omega_2}} \quad ({\rm W}^{-1})$$

in the same units as equation (1.7.3.70).

1.7.3.3.4.2. *SFG ($\omega_s + \omega_p = \omega_i$) with undepletion at ω_p*

$(\omega_s, \omega_p, \omega_i) = (\omega_1, \omega_2, \omega_3)$ or $(\omega_2, \omega_1, \omega_3)$.

The undepleted wave at ω_p, the pump, is mixed in the nonlinear crystal with the depleted wave at ω_s, the signal, in order to generate the idler wave at $\omega_i = \omega_s + \omega_p$. The integrations of the coupled amplitude equations over (X, Y, Z) with $E_s(X, Y, 0) \neq 0$, $E_p(X, Y, 0) \neq 0$, $\partial E_p(X, Y, Z)/\partial Z = 0$ and $E_i(X, Y, 0) = 0$ give

$$P_p(L) = T_p^2 P_p(0) \tag{1.7.3.84}$$

$$P_i(L) = \frac{\omega_i}{\omega_s}P_s(0)\Gamma^2L^2\frac{\sin^2\{\Gamma^2L^2 + [(\Delta k \cdot L)/2]^2\}^{1/2}}{\Gamma^2L^2 + [(\Delta k \cdot L)/2]^2} \tag{1.7.3.85}$$

$$P_s(L) = P_s(0)\left[1 - \frac{\omega_s}{\omega_i}\frac{P_i(L)}{P_s(0)}\right], \tag{1.7.3.86}$$

with $\Delta k = k_i - (k_s + k_p)$ and $\Gamma^2 = [B_s P_p(0)]/w_o^2$, where

$$B_s = \frac{8\pi}{\varepsilon_o c}\frac{2N-1}{N}\frac{d_{\rm eff}^2}{\lambda_s\lambda_i}\frac{T_s T_p T_i}{n_s n_p n_i}.$$

Thus, even if the up-conversion process is phase-matched ($\Delta k = 0$), the power transfers are periodic: the photon transfer efficiency is then 100% for $\Gamma L = (2m + 1)(\pi/2)$, where m is an integer, which allows a maximum power gain ω_i/ω_s for the idler. A nonlinear crystal with length $L = (\pi/2\Gamma)$ is sufficient for an optimized device.

For a small conversion efficiency, *i.e.* ΓL weak, (1.7.3.85) and (1.7.3.86) become

$$P_i(L) \simeq P_s(0)\frac{\omega_i}{\omega_s}\Gamma^2L^2\sin c^2\frac{\Delta k \cdot L}{2} \tag{1.7.3.87}$$

and

$$P_s(L) \simeq P_s(0). \tag{1.7.3.88}$$

The expression for $P_i(L)$ with $\Delta k = 0$ is then equivalent to (1.7.3.83) with $\omega_p = \omega_1$ or ω_2, $\omega_i = \omega_3$ and $\omega_s = \omega_2$ or ω_1.

For example, the frequency up-conversion interaction can be of great interest for the detection of a signal, ω_s, comprising IR radiation with a strong divergence and a wide spectral bandwidth. In this case, the achievement of a good conversion efficiency, $P_i(L)/P_s(0)$, requires both wide spectral and angular acceptance bandwidths with respect to the signal. The double non-criticality in frequency and angle (DNPM) can then be used with one-beam non-critical non-collinear phase matching (OBNC) associated with vectorial group phase matching (VGPM) (Dolinchuk *et al.*, 1994): this corresponds to the equality of the absolute magnitudes and directions of the signal and idler group velocity vectors *i.e.* $\mathrm{d}\omega_i/\mathrm{d}\mathbf{k}_i = \mathrm{d}\omega_s/\mathrm{d}\mathbf{k}_s$.

1.7.3.3.5. *Difference-frequency generation (DFG)*

DFG is defined by $\omega_3 - \omega_1 = \omega_2$ with $E_2(X, Y, 0) = 0$ or $\omega_3 - \omega_2 = \omega_1$ with $E_1(X, Y, 0) = 0$. The DFG phase-matching configurations are given in Table 1.7.3.1. As for SFG, the solutions of system (1.7.3.22) are Jacobian elliptic functions when the incident waves are both depleted. We consider here the simplified situations of undepletion of the two incident waves and depletion of only one incident wave. In the latter, the solutions differ according to whether the circular frequency of the undepleted wave is the highest one, *i.e.* ω_3, or not. We consider the case of plane waves that propagate in a direction without walk-off and we assume a flat energy distribution for the three beams.

1.7.3.3.5.1. *DFG ($\omega_p - \omega_s = \omega_i$) with undepletion at ω_p and ω_s*

$(\omega_s, \omega_i, \omega_p) = (\omega_1, \omega_2, \omega_3)$ or $(\omega_2, \omega_1, \omega_3)$.

The resolution of system (1.7.3.22) with $E_s(X, Y, 0) \neq 0$, $E_p(X, Y, 0) \neq 0$, $\partial E_p(X, Y, Z)/\partial Z = \partial E_s(X, Y, Z)/\partial Z = 0$ and $E_i(X, Y, 0) = 0$, followed by integration over (X, Y), leads to the same solutions as for SFG with undepletion at ω_1 and ω_2, *i.e.* formulae (1.7.3.81), (1.7.3.82) and (1.7.3.83), by replacing ω_1 by ω_s, ω_2 by ω_p and ω_3 by ω_i. A schematic device is given in Fig. 1.7.3.17 by replacing $(\omega_1, \omega_2, \omega_3)$ by $(\omega_1, \omega_3, \omega_2)$ or $(\omega_2, \omega_3, \omega_1)$.

1.7.3.3.5.2. *DFG ($\omega_s - \omega_p = \omega_i$) with undepletion at ω_p*

$(\omega_s, \omega_i, \omega_p) = (\omega_3, \omega_1, \omega_2)$ or $(\omega_3, \omega_2, \omega_1)$.

The resolution of system (1.7.3.22) with $E_s(X, Y, 0) \neq 0$, $E_p(X, Y, 0) \neq 0$, $\partial E_p(X, Y, Z)/\partial Z = 0$ and $E_i(X, Y, 0) = 0$, followed by the integration over (X, Y), leads to the same solutions as for SFG with undepletion at ω_1 or ω_2: formulae (1.7.3.84), (1.7.3.85) and (1.7.3.86).

1.7.3.3.5.3. *DFG ($\omega_p - \omega_s = \omega_i$) with undepletion at ω_p – optical parametric amplification (OPA), optical parametric oscillation (OPO)*

$(\omega_s, \omega_i, \omega_p) = (\omega_1, \omega_2, \omega_3)$ or $(\omega_2, \omega_1, \omega_3)$.

The initial conditions are the same as in Section 1.7.3.3.5.2, except that the undepleted wave has the highest circular frequency. In this case, the integrations of the coupled amplitude equations over (X, Y, Z) lead to

$$P_p(L) = T_p^2 P_p(0), \tag{1.7.3.89}$$

$$P_i(L) = P_s(0)\frac{\omega_i}{\omega_s}\Gamma^2L^2\frac{\sinh^2\{\Gamma^2L^2 - [(\Delta k \cdot L)/2]^2\}^{1/2}}{\Gamma^2L^2 - [(\Delta k \cdot L)/2]^2} \tag{1.7.3.90}$$

and

$$\begin{aligned} P_s(L) &= P_s(0)\left[1 + \frac{\omega_s}{\omega_i}\frac{P_i(L)}{P_s(0)}\right] \\ &= P_s(0)\left(1 + \Gamma^2L^2\frac{\sinh^2\{\Gamma^2L^2 - [(\Delta k \cdot L)/2]^2\}^{1/2}}{\Gamma^2L^2 - [(\Delta k \cdot L)/2]^2}\right) \end{aligned} \tag{1.7.3.91}$$

with $\Delta k = k_p - (k_i + k_s)$ and $\Gamma^2 = [B_i P_p(0)]/w_o^2$, where w_o is the beam radius of the three beams and

$$B_i = \frac{8\pi}{\varepsilon_o c}\frac{2N-1}{N}\frac{d_{\rm eff}^2}{\lambda_s\lambda_i}\frac{T_s T_p T_i}{n_s n_p n_i}.$$

The units are the same as in equation (1.7.3.42).

Equations (1.7.3.90) and (1.7.3.91) show that both idler and signal powers grow exponentially. So, firstly, the generation of the idler is not detrimental to the signal power, in contrast to DFG ($\omega_s - \omega_p = \omega_i$) and SFG ($\omega_s + \omega_p = \omega_i$), and, secondly, the signal power is amplified. Thus DFG ($\omega_p - \omega_s = \omega_i$) combines two interesting functions: generation at ω_i and amplification at ω_s. The last function is called optical parametric amplification (OPA).

The gain of OPA can be defined as (Harris, 1969)

$$G(L) = \left|\frac{P_s(L)}{P_s(0)} - 1\right|. \qquad (1.7.3.92)$$

For example, Baumgartner & Byer (1979) obtained a gain of about 10 for the amplification of a beam at 0.355 μm by a pump at 1.064 μm in a 5 cm long KH_2PO_4 crystal, with a pump intensity of 28 MW cm^{-2}.

According to (1.7.3.91), for $\Delta k^2 L^2/4 \gg \Gamma^2 L^2$, $\sinh^2(im) \rightarrow -\sin^2(m)$ and so the gain is given by

$$G_{\text{small gain}} \simeq \Gamma^2 L^2 \sin c^2\left(\frac{\Delta k \cdot L}{2}\right). \qquad (1.7.3.93)$$

Formula (1.7.3.93) shows that frequencies can be generated around ω_s. The full gain linewidth of the signal, $\Delta\omega_s$, is defined as the linewidth leading to a maximum phase mismatch $\Delta k = 2\pi/L$. If we assume that the pump wave linewidth is negligible, *i.e.* $\Delta\omega_p = 0$, it follows, by expanding Δk in a Taylor series around ω_i and ω_s, and by only considering the first order, that

$$\left|\Delta\omega_s^{\text{small gain}}\right| = \left|\Delta\omega_i^{\text{small gain}}\right| \simeq (2\pi/Lb) \qquad (1.7.3.94)$$

with $b = [1/v_g(\omega_i)] - [1/v_g(\omega_s)]$, where $v_g(\omega) = \partial\omega/\partial k$ is the group velocity.

This linewidth can be termed intrinsic because it exists even if the pump beam is parallel and has a narrow spectral spread.

For type I, the spectral linewidth of the signal and idler waves is largest at the degeneracy: $b = 0$ because the idler and signal waves have the same polarization and so the same group velocity at degeneracy, *i.e.* $\omega_i = \omega_s = \omega_p/2$. In this case, it is necessary to consider the dispersion of the group velocity $\partial^2\omega/\partial^2 k$ for the calculation of $\Delta\omega_s$ and $\Delta\omega_i$. Note that an increase in the crystal length allows a reduction in the linewidth.

For type II, b is never nil, even at degeneracy.

A parametric amplifier placed inside a resonant cavity constitutes an optical parametric oscillator (OPO) (Harris, 1969; Byer, 1973; Brosnan & Byer, 1979; Yang *et al.*, 1993). In this case, it is not necessary to have an incident signal wave because both signal and idler photons can be generated by spontaneous parametric emission, also called parametric noise or parametric scattering (Louisell *et al.*, 1961): when a laser beam at ω_p propagates in a $\chi^{(2)}$ medium, it is possible for pump photons to spontaneously break down into pairs of lower-energy photons of circular frequencies ω_s and ω_i with the total photon energy conserved for each pair, *i.e* $\omega_s + \omega_i = \omega_p$. The pairs of generated waves for which the phase-matching condition is satisfied are the only ones to be efficiently coupled by the nonlinear medium. The OPO can be singly resonant (SROPO) at ω_s or ω_i (Yang *et al.*, 1993; Chung & Siegman, 1993), doubly resonant (DROPO) at both ω_s and ω_i (Yang *et al.*, 1993; Breitenbach *et al.*, 1995) or triply resonant (TROPO) (Debuisschert *et al.*, 1993; Scheidt *et al.*, 1995). Two main techniques for the pump injection exist: the pump can propagate through the cavity mirrors, which allows the smallest cavity length; for continuous waves or pulsed waves with a pulsed duration greater than 1 ns, it is possible to increase the cavity length in order to put two 45° mirrors in the cavity for the pump, as shown in Fig. 1.7.3.18. This second technique allows us to use simpler mirror coatings because they are not illuminated by the strong pump beam.

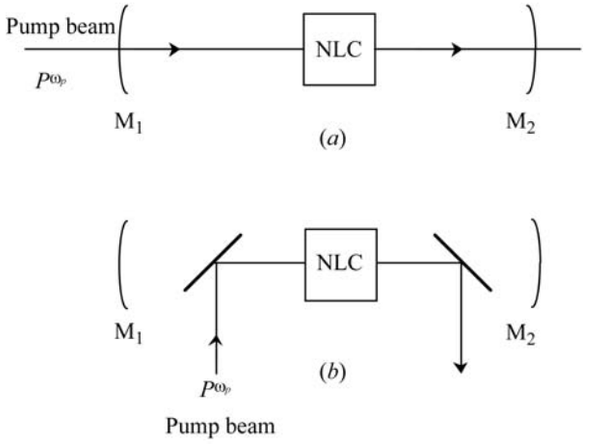

Fig. 1.7.3.18. Schematic OPO configurations. P^{ω_p} is the pump power. (*a*) can be a SROPO, DROPO or TROPO and (*b*) can be a SROPO or DROPO, according to the reflectivity of the cavity mirrors (M_1, M_2).

The only requirement for making an oscillator is that the parametric gain exceeds the losses of the resonator. The minimum intensity above which the OPO has to be pumped for an oscillation is termed the threshold oscillation intensity I_{th}. The oscillation threshold decreases when the number of resonant frequencies increases: $I_{\text{th}}^{\omega_p}$(SROPO) > $I_{\text{th}}^{\omega_p}$(DROPO) > $I_{\text{th}}^{\omega_p}$(TROPO); on the other hand the instability increases because the condition of simultaneous resonance is critical.

The oscillation threshold of a SROPO or DROPO can be decreased by reflecting the pump from the output coupling mirror M_2 in configuration (*a*) of Fig. 1.7.3.18 (Marshall & Kaz, 1993). It is necessary to pump an OPO by a beam with a smooth optical profile because hot spots could damage all the optical components in the OPO, including mirrors and nonlinear crystals. A very high beam quality is required with regard to other parameters such as the spectral bandwidth, the pointing stability, the divergence and the pulse duration.

The intensity threshold is calculated by assuming that the pump beam is undepleted. For a phase-matched SROPO, resonant at ω_s or ω_i, and for nanosecond pulsed beams with intensities that are assumed to be constant over one single pass, $I_{\text{th}}^{\omega_p}$ is given by

$$I_{\text{th}}^{\omega_p} = \frac{1.8}{KL^2(1+\gamma)^2}\left\{\frac{25L}{c\tau} + 2\alpha L + Ln\left[\frac{1}{(1-T)^{1/2}}\right] + Ln(2)\right\}^2. \qquad (1.7.3.95)$$

$K = (\omega_s\omega_i\chi_{\text{eff}}^2)/[2n(\omega_s)n(\omega_i)n(\omega_p)\varepsilon_o c^3]$; L is the crystal length; γ is the ratio of the backward to the forward pump intensity; τ is the $1/e^2$ half width duration of the pump beam pulse; and 2α and T are the linear absorption and transmission coefficients at the circular frequency of the resonant wave ω_s or ω_i. In the nanosecond regime, typical values of $I_{\text{th}}^{\omega_p}$ are in the range 10–100 MW cm^{-2}.

(1.7.3.95) shows that a small threshold is achieved for long crystal lengths, high effective coefficient and for weak linear losses at the resonant frequency. The pump intensity threshold must be less than the optical damage threshold of the nonlinear crystal, including surface and bulk, and of the dielectric coating of any optical component of the OPO. For example, a SROPO using an 8 mm long $KNbO_3$ crystal ($d_{\text{eff}} \simeq 10$ pm V^{-1}) as a nonlinear crystal was performed with a pump threshold intensity of 65 MW cm^{-2} (Unschel *et al.*, 1995): the 3 mm-diameter pump beam was a 10 Hz injection-seeded single-longitudinal-mode Nd:YAG laser at 1.064 μm with a 9 ns pulse of 100 mJ; the SROPO was pumped as in Fig. 1.7.3.18(*a*) with a cavity length of 12 mm, a mirror M_1 reflecting 100% at the signal, from 1.4 to

2 μm, and a coupling mirror M_2 reflecting 90% at the signal and transmitting 100% at the idler, from 2 to 4 μm.

For increasing pump powers above the oscillation threshold, the idler and signal powers grow with a possible depletion of the pump.

The total signal or idler conversion efficiency from the pump depends on the device design and pump source. The greatest values are obtained with pulsed beams. As an example, 70% peak power conversion efficiency and 65% energy conversion of the pump to both signal (λ_s = 1.61 μm) and idler (λ_i = 3.14 μm) outputs were obtained in a SROPO using a 20 mm long KTP crystal ($d_{\rm eff}$ = 2.7 pm V^{-1}) pumped by an Nd:YAG laser (λ_p = 1.064 μm) for eye-safe source applications (Marshall & Kaz, 1993): the configuration is the same as in Fig. 1.7.3.18(*a*) where M_1 has high reflection at 1.61 μm and high transmission at 1.064 μm, and M_2 has high reflection at 1.064 μm and a 10% transmission coefficient at 1.61 μm; the Q-switched pump laser produces a 15 ns pulse duration (full width at half maximum), giving a focal intensity around 8 MW cm^{-2} per mJ of pulse energy; the energy conversion efficiency from the pump relative to the signal alone was estimated to be 44%.

OPOs can operate in the continuous-wave (cw) or pulsed regimes. Because the threshold intensity is generally high for the usual nonlinear materials, the cw regime requires the use of DROPO or TROPO configurations. However, cw-SROPO can run when the OPO is placed within the pump-laser cavity (Ebrahimzadeh *et al.*, 1999). The SROPO in the classical external pumping configuration, which leads to the most practical devices, runs very well with a pulsed pump beam, *i.e.* Q-switched laser running in the nanosecond regime and mode-locked laser emitting picosecond or femtosecond pulses. For nanosecond operation, the optical parametric oscillation is ensured by the same pulse, because several cavity round trips of the pump are allowed during the pulse duration. It is not possible in the ultrafast regimes (picosecond or femtosecond). In these cases, it is necessary to use synchronous pumping: the round-trip transit time in the OPO cavity is taken to be equal to the repetition period of the pump pulse train, so that the resonating wave pulse is amplified by successive pump pulses [see for example Ruffing *et al.* (1998) and Reid *et al.* (1998)].

OPOs are used for the generation of a fixed wavelength, idler or signal, but have potential for continuous wavelength tuning over a broad range, from the near UV to the mid-IR. The tuning is based on the dispersion of the refractive indices with the wavelength, the direction of propagation, the temperature or any other variable of dispersion. More particularly, the crystal must be phase-matched for DFG over the widest spectral range for a reasonable variation of the dispersion parameter to be used. Several methods are used: variation of the pump wavelength at a fixed direction, fixed temperature *etc.*; rotation of the crystal at a fixed pump wavelength, fixed temperature *etc.*; or variation of the crystal temperature at a fixed pump wavelength, fixed direction *etc.*

We consider here two of the most frequently encountered methods at present: for birefringence phase matching, angle tuning and pump-wavelength tuning; and the case of quasi phase matching.

(i) *OPO with angle tuning*.

The function of a tunable OPO is to generate the signal and idler waves over a broad range, $\Delta\omega_s$ and $\Delta\omega_i$, respectively, from a fixed pump wave at ω_p. The spectral shifts $\Delta\omega_s = \omega_s^+ - \omega_s^-$ and $\Delta\omega_i = \omega_i^+ - \omega_i^-$ are obtained by rotating the nonlinear crystal by an angle $\Delta\alpha = \alpha^+ - \alpha^-$ in order to achieve phase matching over the spectral range considered: $\omega_p n(\omega_p, \alpha) = \omega_i n(\omega_i, \alpha) + \omega_s n(\omega_s, \alpha)$ with $\omega_p = \omega_i + \omega_s$ from $(\omega_s^+, \omega_i^-, \alpha^\pm)$ to $(\omega_s^-, \omega_i^+, \alpha^\mp)$, where $(-)$ and $(+)$, respectively, denote the minimum and maximum values of the data considered. Note that $\Delta\omega_s = -\Delta\omega_i$ and so $(\Delta\lambda_i/\lambda_i^+\lambda_i^-) = -(\Delta\lambda_s/\lambda_s^+\lambda_s^-)$ if the spectral bandwidth of the pump, $\delta\omega_p$, is zero.

In the case of parallelepipedal nonlinear crystals, the tuning rate $\Delta\omega_{i,s}/\Delta\alpha$ has to be high because $\Delta\alpha$ cannot exceed about 30° of arc, *i.e.* 15° on either side of the direction normal to the plane surface of the nonlinear crystal: in fact, the refraction can lead to an attenuation of the efficiency of the parametric interaction for larger angles. For this reason, a broad-band OPO necessarily requires angular critical phase matching (CPM) directions over a broad spectral range. However, the angular criticality is detrimental to the spectral stability of the signal and idler waves with regard to the pointing fluctuations of the pump beam: a pointing instability of the order of 100 μrad is considered to be acceptable for OPOs based on KTP or BBO crystals. Fig. 1.7.3.19 shows the phase-matching tuning curves $\lambda_i(\alpha)$ and $\lambda_s(\alpha)$ for (*a*) BBO pumped at λ_p = 355 nm and (*b*) KTP pumped at λ_p = 1064 nm, where $\alpha = \theta$ or φ is an internal angle: the calculations were carried out using the refractive indices given in Kato (1986) for BBO and in Kato (1991) for KTP.

The divergence of the pump beam may increase the spectral bandwidths $\delta\omega_s$ and $\delta\omega_i$: the higher the derivatives $\partial\lambda_{i,s}/\partial\alpha$ are, the higher the spectral bandwidths for a given pump divergence are. Furthermore, $\partial\lambda_{i,s}/\partial\alpha$ vary as a function of the phase-matching angle α. The derivative is a maximum at the degeneracy $\lambda_i = \lambda_s = 2\lambda_p$, when the idler and signal waves are identically polarized: this is the case for BBO as shown in Fig. 1.7.3.19(*a*). We give another example of a type-I BBO OPO pumped at 308 nm by a narrow-band injection-seeded ultraviolet XeCl excimer laser (Ebrahimzadeh *et al.*, 1990): the spectral bandwidth, expressed in cm^{-1} ($\partial\lambda_{i,s}/\lambda_{i,s}^2 = \partial\omega_{i,s}/2\pi c$), varies from $\sim$78 cm^{-1} to $\sim$500 cm^{-1} for a crystal length of 1.2 cm, corresponding to a signal bandwidth $\delta\lambda_s \simeq$ 1.8 nm at 480 nm and $\delta\lambda_s \simeq$ 18 nm at 600 nm, respectively. The degeneracy is not a particular situation with respect to the derivative of the phase-matching curve when the idler and signal waves are orthogonally polarized as shown in Fig. 1.7.3.19(*b*) with the example of KTP.

The way currently used for substantial reduction of the spectral bandwidth is to introduce bandwidth-limiting elements in the OPO cavity, such as a grazing grating associated with a tuning mirror reflecting either the signal or the idler according to the chosen resonant wavelength. The rotations of the nonlinear crystal and of the restricting element have to be synchronized in order to be active over all the wavelength range generated. Narrow bandwidths of about 0.1 cm^{-1} can be obtained in this way, but the gain of such a device is low. High energy and narrow spectral bandwidth can be obtained at the same time by the association of two OPOs: an OPO pumped at ω_p and without a restricting element inside the cavity is seeded by the idler or signal beam emitted by a narrow spectral bandwidth OPO also pumped at ω_p.

The disadvantages of parallelepipedal crystals can be circumvented by using a nonlinear crystal cut as a cylindrical plate, with the cylinder axis orthogonal to the OPO cavity axis and to the plane of the useful phase-matching directions (Boulanger *et al.*, 1999; Pacaud *et al.*, 2000; Fève, Pacaud *et al.*, 2002). Such a geometry allows us to consider any phase-matching range by rotation of the cylinder around its revolution axis. It is then possible to use interactions with a weak angular tuning rate to reduce the spectral bandwidth and increase the stability of the generated beams. Moreover, the propagation of the beams is at normal incidence for any direction, so collinear phase matching can be maintained, leading to better spatial and spectral transverse profiles. Because of the cylindrical geometry of the nonlinear crystal, it is necessary to focus the pump beam and to collect the signal and idler beams with cylindrical lenses. The cavity mirrors, plane or cylindrical, are then placed between the nonlinear crystal and the lenses. The diameter of the crystal being about a few tenths of a millimetre, the associated focal distance is short, *i.e.* a few millimetres, which leads to a strong spatial filtering effect, preventing the oscillation of beams with a quality factor M^2 bigger than about 1.5.

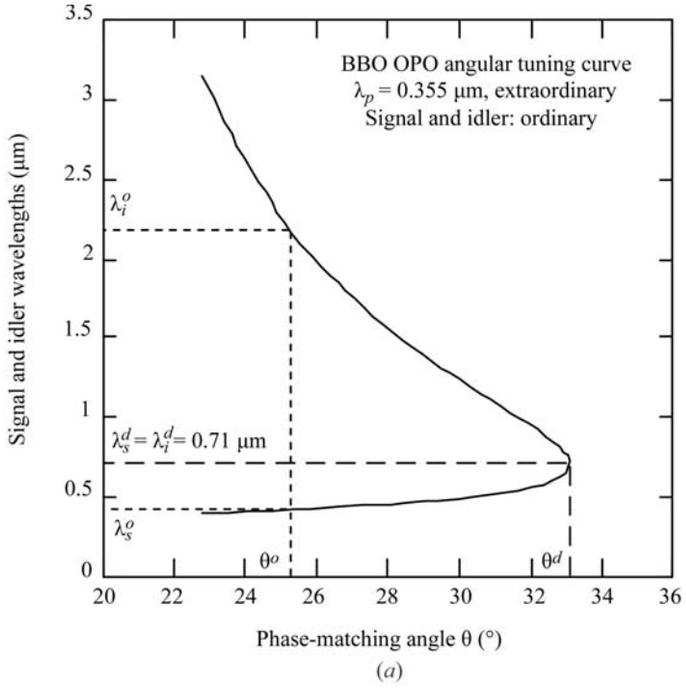

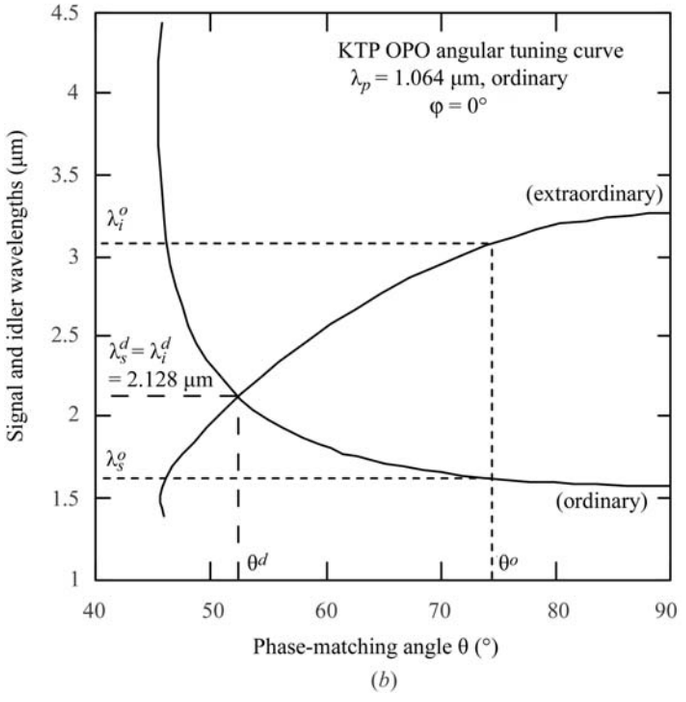

Fig. 1.7.3.19. Calculated angular tuning curves. θ and φ are the spherical coordinates of the phase-matching directions. θ^d is the phase-matching angle of the degeneracy process ($\lambda_i^d = \lambda_s^d = 2\lambda_p$). λ_i^o and λ_s^o are the idler and signal wavelengths, respectively, generated at θ^o. Ordinary and extraordinary refer to the polarization.

(ii) *OPO with a tuning pump*.

The nonlinear crystal is fixed and the pump frequency can vary over $\Delta\omega_p$, leading to a variation of the signal and idler frequencies such that $\Delta\omega_i + \Delta\omega_s = \Delta\omega_p$.

In Fig. 1.7.3.20, the example of *N*-(4-nitrophenyl)-L-propinol (NPP) pumped between 610 and 621 nm is shown (Ledoux *et al.*, 1990; Khodja *et al.*, 1995*a*). The phase-matching curve $\lambda_{i,s}(\lambda_p)$ is calculated from the Sellmeier equations of Ledoux *et al.* (1990) for the case of identical polarizations for the signal and idler waves. The tuning rate is a maximum at the degeneracy, as for angular tuning with identical polarizations.

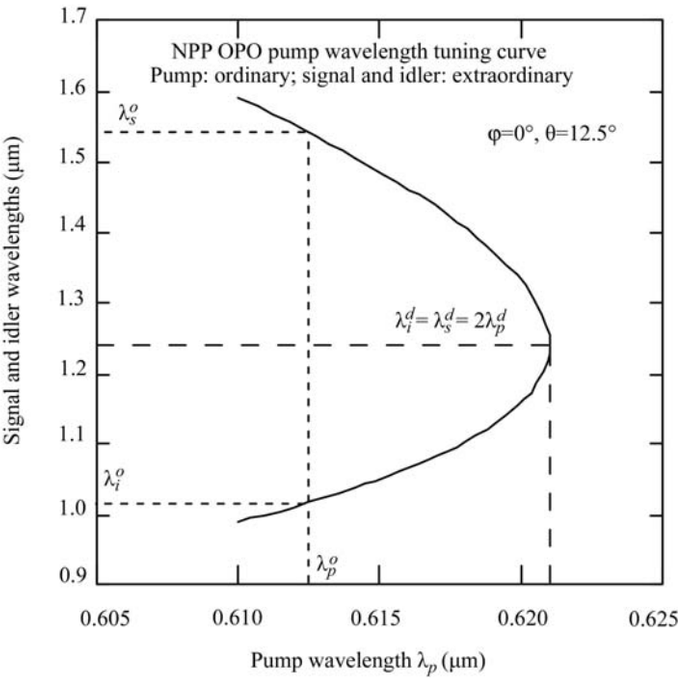

Fig. 1.7.3.20. Calculated pump wavelength tuning curve. λ_p^d is the pump wavelength leading to degeneracy for the direction considered ($\theta = 12.5$, $\varphi = 0°$). Ordinary and extraordinary refer to the polarization.

For any configuration of polarization, the most favourable direction of propagation of an OPO with a tuning pump is a principal axis of the index surface, because the phase matching is angular non-critical and so wavelength critical. In this optimal situation, the OPO has a low sensitivity to the divergence and pointing stability of the pump beam; furthermore, the walk-off angle is nil, which provides a higher conversion efficiency.

(iii) *Quasi-phase-matched OPO with a tunable periodicity*.

In a QPM device, the interacting frequencies are fixed by the frequency dispersion of the birefringence of the nonlinear material and by the periodicity of the grating. A first possibility is to fabricate a series of gratings with different periodicities in the same nonlinear crystal; the translation of this crystal with respect to the fixed pump beam allows us to address the different gratings and thus to generate different couples (ω_s, ω_i). Because the tuning is obtained in discrete steps, it is necessary to combine temperature or angle tuning with the translation of the sample in order to interpolate smoothly between the steps. For example, a device based on a periodically poled $LiNbO_3$ (ppLN) crystal with a thickness of 0.5 mm and a length along the periodicity vector of 1 cm has been developed (Myers *et al.*, 1996). A total of 25 gratings with periods between 26 and 32 μm were realized in 0.25 μm increments. The OPO was pumped at 1.064 μm and generated a signal between 1.35 and 1.98 μm, with the corresponding idler between 4.83 and 2.30 μm.

Fan-shaped gratings have been demonstrated as an alternative approach for continuous tuning (Powers *et al.*, 1998). However, such a structure has the disadvantage of introducing large spectral heterogeneity to the generated beams, because the grating period is not constant over the pump beam diameter.

Finally, the most satisfactory alternative for continuous tuning is the use of a cylindrical crystal with one single grating (Fève *et al.*, 2001). The variations of the signal and idler wavelengths are then obtained by rotation of the cylinder around its revolution axis, which is orthogonal to the OPO cavity axis and to the plane containing the frame vector Λ. For a direction of propagation making an angle α with Λ, the effective period of the grating as seen by the collinear interacting wavevectors is $\Lambda_\alpha = (\Lambda/\cos\alpha)$, leading to a continuous spectral tuning. For example, a rotation over an α range of 26° of a ppKTP cylinder pumped at 1064 nm

leads to a signal tuning range of 520 nm, between 1515 and 2040 nm, while the corresponding idler is tuned over 1340 nm, between 2220 and 3560 nm.

For an overview of OPO and OPA, the reader may refer to the following special issues of the *Journal of the Optical Society of America B*: (1993), **10**(9), 1656–1794; (1993), **10**(11), 2148–2239 and (1995), **12**(11), 2084–2310; and to the *Handbook of Optics* devoted to OPO (Ebrahimzadeh & Dunn, 2000).

1.7.4. Determination of basic nonlinear parameters

We review here the different methods that are used for the study of nonlinear crystals.

1.7.4.1. *Phase-matching directions and associated acceptance bandwidths*

The very early stage of crystal growth of a new material usually provides a powder with particle sizes less than 100 μm. It is then impossible to measure the phase-matching loci. Nevertheless, careful SHG experiments performed on high-quality crystalline material may indicate whether the SHG is phase-matched or not by considering the dependence of the SHG intensity on the following parameters: the angle between the detector and the direction of the incident fundamental beam, the powder layer thickness, the average particle size and the laser beam diameter (Kurtz & Perry, 1968). However, powder measurements are essentially used for the detection in a simple and quick way of noncentrosymmetry of crystals, this criterion being necessary to have a nonzero $\chi^{(2)}$ tensor (Kurtz & Dougherty, 1978). They also allow, for example, the measurement of the temperature of a possible centrosymmetric/noncentrosymmetric transition (Marnier *et al.*, 1989).

For crystal sizes greater than few hundred μm, it is possible to perform direct measurements of phase-matching directions. The methods developed at present are based on the use of a single crystal ground into an ellipsoidal (Velsko, 1989) or spherical shape (Marnier & Boulanger, 1989; Boulanger, 1989; Boulanger *et al.*, 1998); a sphere is difficult to obtain for sample diameters less than 2 mm, but it is the best geometry for large numbers and accurate measurements because of normal refraction for every chosen direction of propagation. The sample is oriented using X-rays, placed at the centre of an Euler circle and illuminated with fixed and appropriately focused laser beams. The experiments are usually performed with SHG of different fundamental wavelengths. The sample is rotated in order to propagate the fundamental beam in different directions: a phase-matching direction is then detected when the SHG conversion efficiency is a maximum. It is then possible to describe the whole phase-matching cone with an accuracy of 1°. A spherical crystal also allows easy measurement of the walk-off angle of each of the waves (Boulanger *et al.*, 1998). It is also possible to perform a precise observation and study of the internal conical refraction in biaxial crystals, which leads to the determination of the optic axis angle $V(\omega)$, given by relation (1.7.3.14), for different frequencies (Fève *et al.*, 1994).

Phase-matching relations are often poorly calculated when using refractive indices determined by the prism method or by measurement of the critical angle of total reflection. Indeed, all the refractive indices concerned have to be measured with an accuracy of 10^{-4} in order to calculate the phase-matching angles with a precision of about 1°. Such accuracies can be reached in the visible spectrum, but it is more difficult for infrared wavelengths. Furthermore, it is difficult to cut a prism of few mm size with plane faces.

If the refractive indices are known with the required accuracy at several wavelengths well distributed across the transparency region, it is possible to fit the data with a Sellmeier equation of the following type, for example:

$$n_i^2(\lambda) = A_i + \frac{B_i\lambda^2}{\lambda^2 - C_i} + D_i\lambda^2. \qquad (1.7.4.1)$$

n_i is the principal refractive index, where $i = o$ (ordinary) and e (extraordinary) for uniaxial crystals and $i = x$, y and z for biaxial crystals.

It is then easy to calculate the phase-matching angles (θ_{PM}, φ_{PM}) from (1.7.4.1) using equations (1.7.3.27) or (1.7.3.29) where the angular variation of the refractive indices is given by equation (1.7.3.6).

The measurement of the variation of intensity of the generated beam as a function of the angle of incidence can be performed on a sphere or slab, leading, respectively, to internal and external angular acceptances. The thermal acceptance is usually measured on a slab which is heated or cooled during the frequency conversion process. The spectral acceptance is not often measured, but essentially calculated from Sellmeier equations (1.7.4.1) and the expansion of Δk in the Taylor series (1.7.3.43) with $\xi = \lambda$.

1.7.4.2. *Nonlinear coefficients*

The knowledge of the absolute magnitude and of the relative sign of the independent elements of the tensors $\chi^{(2)}$ and $\chi^{(3)}$ is of prime importance not only for the qualification of a new crystal, but also for the fundamental engineering of nonlinear optical materials in connection with microscopic aspects.

However, disparities in the published values of the nonlinear coefficients of the same crystal exist, even if it is a well known material that has been used for a long time in efficient devices (Eckardt & Byer, 1991; Boulanger, Fève *et al.*, 1994). The disagreement between the different absolute magnitudes is sometimes a result of variation in the quality of the crystals, but mainly arises from differences in the measurement techniques. Furthermore, a considerable amount of confusion exists as a consequence of the difference between the conventions taken for the relation between the induced nonlinear polarization and the nonlinear susceptibility, as explained in Section 1.7.2.1.4.

Accurate measurements require mm-size crystals with high optical quality of both surface and bulk.

1.7.4.2.1. *Non-phase-matched interaction method*

The main techniques used are based on non-phase-matched SHG and THG performed in several samples cut in different directions. The classical method, termed the Maker-fringes technique (Jerphagnon & Kurtz, 1970; Herman & Hayden, 1995), consists of the measurement of the harmonic power as a function of the angle between the fundamental laser beam and the rotated slab sample, as shown in Fig. 1.7.4.1(*a*).

The conversion efficiency is weak because the interaction is non-phase-matched. In normal incidence, the waves are collinear and so formulae (1.7.3.42) for SHG and (1.7.3.80) for THG are valid. These can be written in a more convenient form where the coherence length appears:

$$\begin{aligned} P^{n\omega}(L) &= A^{n\omega}[P^{\omega}(0)]^n (d_{\text{eff}}^{n\omega} \cdot l_c^{n\omega})^2 \sin^2(\pi L/2l_c^{n\omega}) \\ l_c^{2\omega} &= (\pi c/\omega)(2n_3^{2\omega} - n_1^{\omega} - n_2^{\omega})^{-1} \\ l_c^{3\omega} &= (\pi c/\omega)(3n_4^{3\omega} - n_1^{\omega} - n_2^{\omega} - n_3^{\omega})^{-1}. \end{aligned} \qquad (1.7.4.2)$$

The coefficient $A^{n\omega}$ depends on the refractive indices in the direction of propagation and on the fundamental beam geometry: $A^{2\omega}$ and $A^{3\omega}$ can be easily expressed by identifying (1.7.4.2) with (1.7.3.42) and (1.7.3.80), respectively.

When the crystal is rotated, the harmonic and fundamental waves are refracted with different angles, which leads to a variation of the coherence length and consequently to an oscillation of the harmonic power as a function of the angle of incidence, α, of the fundamental beam. Note that the oscillation